Infrared Temperature Measurement of the Laminar Wake of a Hypersonic Sphere

LEE A. YOUNG*
Avco-Everett Research Laboratory, Everett, Mass.

The temperature of the laminar wake of a 0.22-in.-diam nylon spherical projectile traveling at 13,000 fps in a ballistic range filled with 95% N_2 and 5% CO_2 has been measured by observing the infrared radiation from the CO_2 with a gold-doped germanium infrared detector and a 4.39-μ narrow-band filter. The results are compared with theoretical wake temperatures calculated by a two-step procedure. First, the cooling of the shock-heated gas as it expanded to ambient pressure was calculated by a streamtube chemistry program (developed by Lin and Teare). Subsequently, a simple heat conduction calculation was carried out. In the region from 50 to 400 body diameters behind the sphere the experimental CO_2 vibrational temperatures (determined by fitting the radiation measurements with gaussian temperature profiles) agree with the calculated translational temperatures within the scatter of the data. For example, at 200 body diameters the measurements give 1230°K on the centerline while the theoretical temperature is 1410°K. Nearer the body the experimental values are as much as 600°K higher than calculated; a possible explanation for the discrepancy is discussed in the text.

I. Introduction

THIS paper describes the development of the use of infrared radiation for the measurement of temperatures in the wakes of hypersonic projectiles fired in a ballistic range.

Sufficient quantities of infrared radiators, such as NO, should be produced by a body traveling at re-entry velocity in air in a ballistic range, so that the radiation from the wake could be detected with instruments of sufficient sensitivity. In earlier studies,[1, 2] however, little infrared air radiation from the wake has been seen, even when integrated over broad spectral regions, probably due to the small solid angle of the optical systems used. In addition, the maximum speeds available on many ballistic ranges are less than re-entry velocities.

To overcome these difficulties, 5% CO_2 was added to the gas filling of a ballistic range, and an infrared detecting system having an aperture of relatively large solid angle was built. The system included a narrow bandpass interference filter through which part of the 4.3-μ vibrational-rotational spectral band of CO_2 was detected. With this arrangement, wake radiation was observed out to 2000 body diameters behind a spherical projectile traveling at 13,000 fps, and signal-to-noise ratios up to 25 to 1 were achieved. Temperatures were obtained from absolute intensity measurements in this one-color technique; the data were fitted with gaussian radial temperature profiles whose widths and heights were adjustable parameters.

Observation of the radiation from a single species permitted the intensity measurements to be analyzed in a more quantitative fashion than is possible in photographic and radiometric ballistic range experiments[3, 4] that use little spectral resolution.

Received June 18, 1964; revision received January 7, 1965. This work was jointly supported by the Bell Telephone Laboratories, Inc., Contract No. 600767, under Army Missile Command Prime Contract No. DA-30-069-ORD-1955; by the Advanced Research Projects Agency, monitored by the Army Missile Command, under Contract No. DA-19-020-AMC-0210 (part of Project DEFENDER); and by the Ballistic Systems Division of the Air Force Systems Command under Contract No. AF 04(694)-414. The assistance of Morton Camac at the beginning of this experiment and the advice and encouragement of Peter Rose throughout the work are gratefully acknowledged.

* Principal Research Scientist.

This method is useful over the temperature range of 800° to 3000°K and was appropriate to the relatively low wake temperatures encountered at the projectile velocity used. This approach may be contrasted to that of Hooker,[5] who has used visible radiation from sodium D lines to measure temperatures in the range of 3300° to 4500°K in the relatively near wake of a sphere traveling at about 20,000 fps. Since the CO_2 radiation is generally a rapidly varying function of temperature, temperatures determined from radiation measurements can be less affected by errors in pressure estimates than are temperatures derived from density measurements.[6]

To check the accuracy of the measurements and to assist in their interpretation, theoretical wake temperatures are calculated, and the dissociation, radiation, and vibrational relaxation of CO_2 are discussed. A somewhat more comprehensive account of this work may be found in an earlier report.[7]

II. Experimental

In this initial study of the infrared technique, the following experimental conditions in the ballistic range were chosen in order to simplify the interpretation of the experiment: the projectile was a 0.22-in.-diam nylon sphere; the total pressure was 10 mm Hg; the average velocity was 13,000 fps (spread: 11,600 to 13,500 fps); and the gas filling was 5% CO_2, 95% N_2. The use of a spherical projectile was appropriate for a first test of the infrared technique, because its wake is dominated by the inviscid flow field, which can be readily calculated from the shape of the bow shock. At the low pressure used, the wake is laminar.[8] Because the electric

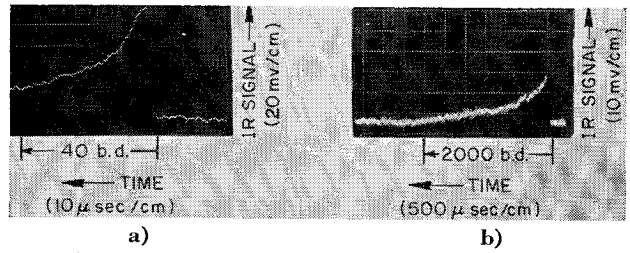

a) b)

Fig. 1 Oscilloscope photographs of the output of the infrared detector. In b, the trace goes off scale at the beginning of the sweep.

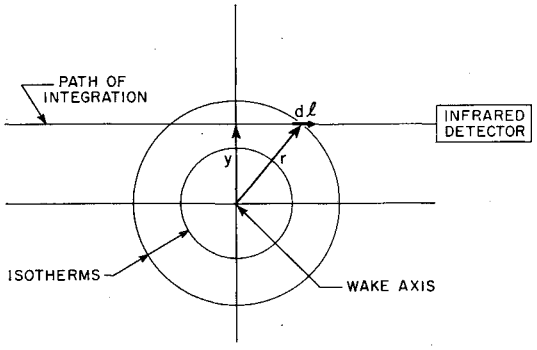

Fig. 2 Geometry for calculation of infrared radiation from the wake. The infrared detector looks through regions of varying temperature, given by $T(r)$. y is a Cartesian coordinate, and r is a cylindrical coordinate.

arc-driven light gas gun was operated at less than its maximum velocity, the nitrogen filling of the range did not dissociate appreciably. (Oxygen was excluded because of its greater dissociation rate.)

A gold-doped germanium infrared detector (Westinghouse type 812) was used. It has a specific detectivity (D^*) of 3×10^9 cm-cps$^{1/2}$/w. An optical system, which included an f/1.3 spherical mirror, produced a 2.5- $\times$ 2.5-mm image of the detector's sensitive element at the center of the ballistic range. From that point, the optical system subtended a solid angle of 0.09 sr. The detector output was connected to a low-noise transistorized amplifier.

A narrow bandpass interference filter, obtained from Optical Coating Laboratory, Inc., was placed in front of the detector. The bandpass of this filter was centered at 4.39 μ, just outside the absorption band of room temperature CO_2, and had a width at half maximum of 0.1 μ.

This infrared detecting system was calibrated both with and without the interference filter using a blackbody source. The responsivity of the detector at 4.39 μ was determined without the filter using the curve of relative spectral response measured by the manufacturer. The result of this determination agreed with the direct determination of narrow band responsivity using the filter within 13%. Individual calibrations of either type were consistent within $\pm 3\%$ during a seven-week period. The detector was found to be linear to 3%. The peak-to-peak noise level of the over-all infrared system corresponded to a radiance of 1.5×10^{-5} w/cm^2-sr.

Two type 6291 photomultipliers located 1.38 ft apart viewed the visible radiation from the projectile through pairs of 0.010-in. slits. These photomultipliers served to determine the projectile velocity, and the time of arrival of the sphere at the infrared detector.

On the side of the ballistic range opposite the infrared detector was a standard Crown Graphic camera whose shutter was left open during the flight of the projectile. The projectile thus left a luminous streak on the film. Fiducial marks at the infrared detector, imaged at the center of the ballistic range, also appeared on the film indicating the distance between the axis of the wake and the axis of the infrared system. The height of the projectile in the ballistic range had a total scatter from run to run of 2 cm which allowed a convenient scan across the wake. Further indication of the projectile trajectory as well as some indication of the condition of the projectile and of accompanying diaphragm fragments, if any, was given by a 0.002-in. brass shim stock target at the end of the range.

Examples of oscillograms of the output of the infrared detector are shown in Fig. 1. In Fig. 1a, taken with a fast sweep speed, the fast rise of the trace indicates the short response time of the infrared system. In Fig. 1b, taken at slower sweep speed, the infrared signal can be seen for a distance of 2000 body diameters behind the projectile. There is a bump in the trace at about 370 body diameters which is probably due to reflection of the bow shock from the walls of the ballistic range back to its center. The noise level is low enough to permit reasonable intensity measurements out to this point. By using three oscilloscopes with different sweep speeds and sensitivities a complete radiation history was obtained for each shot. Time scales were converted to distance scales using the measured velocity.

Each of these radiation histories had a different value of y, the distance between the wake axis and the infrared detector optical axis. (The geometry is shown in Fig. 2.) By cross-plotting, a series of radiation profiles for various distances downstream behind the projectile was obtained. These are of the form $N(y)$, where N is the radiance of the wake in w/cm^2-sr. Examples of these radiation profiles are shown in Fig. 3 for $X/D = 20$ and in Fig. 4 for $X/D = 200$. (Here X is the distance behind the projectile and D is its diameter.) The scatter of the data is reasonably small, considering that each point represents a separate shot on the ballistic range. The theoretical curves that also appear on these figures are derived in the following sections.

III. Theoretical

The temperature of the laminar wake has been calculated by the two-step procedure developed by Feldman.[9] From the bow shock to the point at which ambient pressure is reached, the flow field is dominated by expansion, and diffusion is ignored. The remainder of the wake is a constant pressure region in which diffusion is dominant.

The error introduced by the neglect of diffusion in the expansion region has been considered by Lykoudis.[10] He determined that the centerline enthalpy may be calculated with

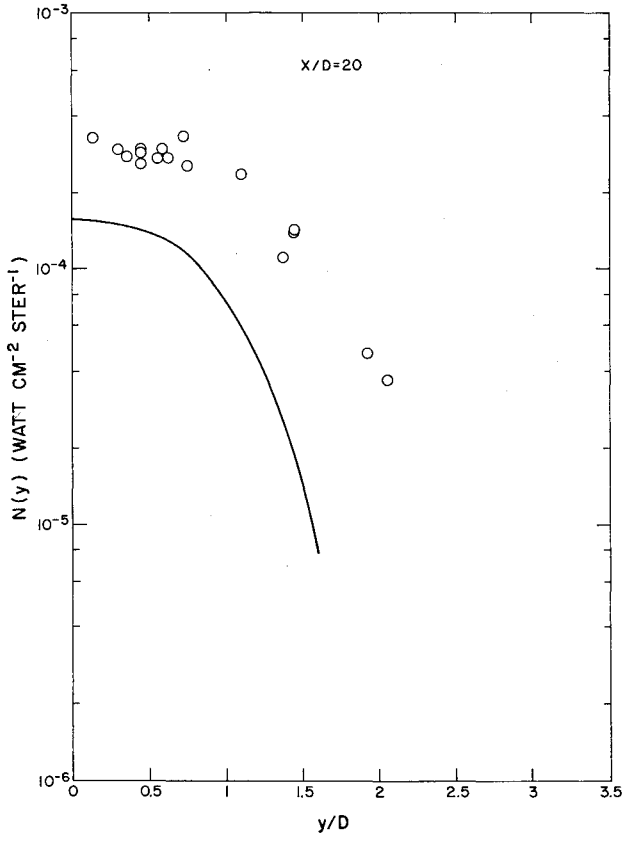

Fig. 3 Infrared radiance at 20 body diameters behind the sphere. y is the lateral distance between the wake axis and the axis of the infrared optical system, and D is the diameter of the sphere. The solid line is a theoretical calculation.

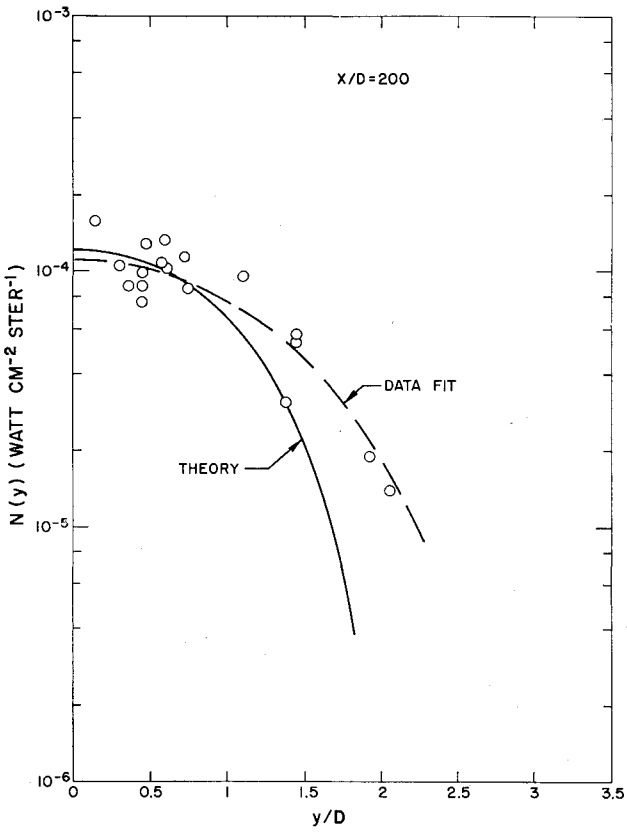

Fig. 4 Infrared radiance at 200 body diameters behind the sphere.

sufficient accuracy using this separation if the parameter Re/M^2 satisfies the condition $Re/M^2 \geq 25$, where Re is the Reynolds number based on sphere radius and freestream conditions, and M is the Mach number. For our case, the values are $Re = 9600$ and $M = 11.8$, so $Re/M^2 = 69$, and the expansion/diffusion split is justified. Other approximations made were: 1) the neglect of the sphere boundary layer on the wake (the ratio of viscous drag to pressure drag of a sphere is less than 0.05), and 2) the neglect of the ablation of the nylon pellet which, although dominating the visible wake, should have little influence in the infrared.

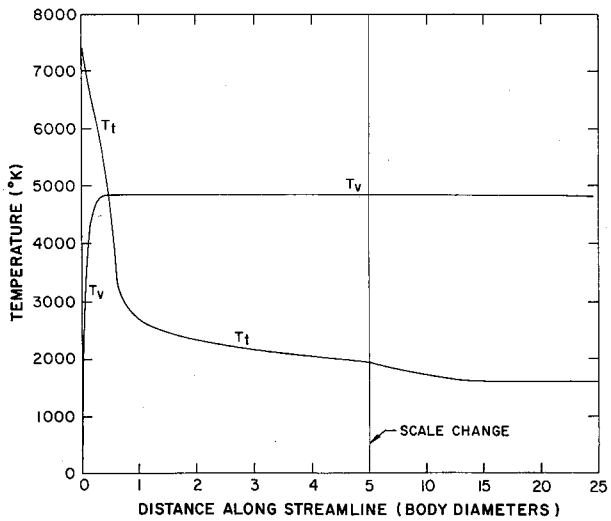

Fig. 5 Translational temperature (T_t) and vibrational temperature (T_v) of nitrogen on the centerline streamline as functions of the distance along the streamline from the bow shock.

The shape of the bow shock used in the present calculation was obtained from a schlieren photograph of unusually good quality by Lobb[11] of a sphere traveling at 17,315 fps, and from a shadowgraph of a sphere at 15,250 fps taken in 1961 at the Avco-Everett Research Laboratory. This shock shape is also consistent with that calculated by Feldman.[9]

Knowing the angle of the shock wave as a function of distance from the axis, we calculated the temperature, pressure, density, and velocity behind the shock wave from the Rankine-Hugoniot equations for pure nitrogen. The effect of CO_2 was assumed negligible.

A. Wake Cooling in the Expansion Region

The cooling of the gas as it expands behind the bow shock was determined by means of a computer program[12] that calculated aerodynamic and chemical processes in air along a streamtube. The required inputs to this program are the conditions at the beginning of a streamline (starting just behind the bow shock) and the pressure variation along the streamline. This pressure distribution is assumed to be unaffected by the details of the chemical process, which the program calculates. Diffusion normal to the streamlines is neglected. The program computes all required aerophysical variables along the streamline as functions of distance and time, including translational temperature, vibrational temperature, and atomic and molecular concentrations of air components.

Six streamlines were followed out to ambient pressure. A gas consisting of 100% N_2 was assumed. The pressure distribution was obtained by fairing a Newtonian pressure function at the front of the sphere to Lukasiewicz's correlation[13] of experimental measurements at $M = 6$ to 8 and detailed calculations at $M = 15$ to 19 of pressure decay behind axisymmetric bodies. According to this correlation, ambient pressure should be reached by 20 body diameters behind the sphere. The radial distance from the wake axis to the ends of the streamlines was determined from the conservation of mass. One result of these calculations was that only 0.03% of the nitrogen dissociates along the centerline streamline (for our low velocity and pressure), with even less dissociation off the axis.

Nitrogen molecules reach vibrational equilibrium in a short distance at the high temperatures, high pressures, and reduced particle speeds that occur just behind the blunt part of the bow shock. But as the gas expands, cools, and accelerates, the characteristic distance for vibrational relaxation increases by a factor of 10^5, so that, in the time scale of this experiment, nitrogen vibration becomes frozen.

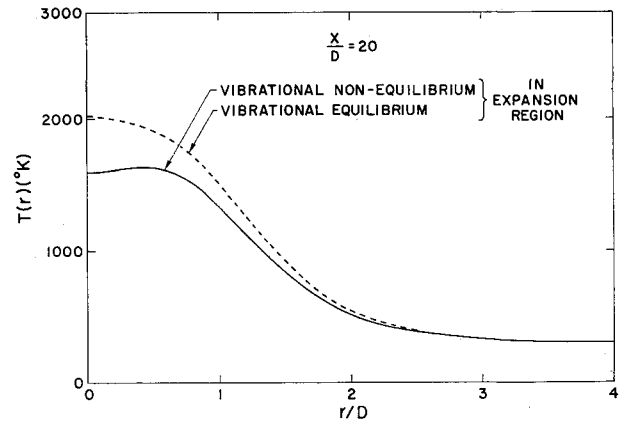

Fig. 6 Temperature profiles at the point where the pressure has decayed to ambient value. The solid curve is for nonequilibrium of nitrogen vibration in the expansion region; the dotted curve is for nitrogen vibrational equilibrium. r is the distance from the wake axis (see Fig. 2).

Nitrogen vibrational and translational temperature histories calculated for the centerline streamtube are plotted in Fig. 5. The vibrational temperature rises rapidly at first and then freezes at a level high enough to depress the translational temperature significantly compared with the equilibrium value.

The entire profile of translational temperature obtained from this calculation is shown as the solid curve in Fig. 6. There is an off-axis peak in this curve because off the axis the excitation of nitrogen vibration is slower, and relatively less energy is frozen out in vibration. (It is possible that the nitrogen is strongly coupled to the vibration of the CO_2, as discussed below. If the CO_2 is a very efficient catalyst for relaxation of nitrogen vibration, then the equilibrium temperature distribution shown by the dotted curve in Fig. 6 would result.)

B. Wake Cooling in the Diffusion Region

The cooling of the laminar wake after expansion to ambient pressure is governed by the heat conduction equation

$$\frac{1}{r}\frac{\partial}{\partial r}\left(rk\frac{\partial T}{\partial r}\right) = \rho c_p \frac{\partial T}{\partial t}$$

in which r is the distance from the wake axis (see Fig. 2), k is the thermal conductivity (which is a function of temperature), ρ is the total gas density, c_p is the specific heat at constant pressure, and the time t refers to events in the history of a given fluid particle in the wake. We may substitute into this equation: 1) the ideal gas law $p_\infty = \rho RT$, in which p_∞ is the total ambient pressure and R is the gas constant for nitrogen, 2) $u = dX/dt$, the velocity of the wake relative to the projectile, which was set at a constant value $u = 0.9u_\infty$ in the diffusion region on the basis of the calculations described previously, and 3) the specific heat for frozen nitrogen vibration given by $c_p/R = \frac{7}{2}$. Combining these expressions we obtain

$$\frac{1}{r}\frac{\partial}{\partial r}\left(rk\frac{\partial T}{\partial r}\right) = 3.15\,\frac{u_\infty p_\infty}{T}\frac{\partial T}{\partial X} \qquad (1)$$

Values of k as a function of temperature were taken from a calculation by Hansen.[14]

In taking a constant value for u, we have neglected the variation of gas velocity with r and X; the viscous conversion of shearing motion into heat has not been taken into account. Feldman[9] has shown that little error is introduced by neglect of these effects.

Equation (1) was converted into a difference equation and integrated using the solid curve in Fig. 6 as an initial condition. No assumption was made about the form of the initial

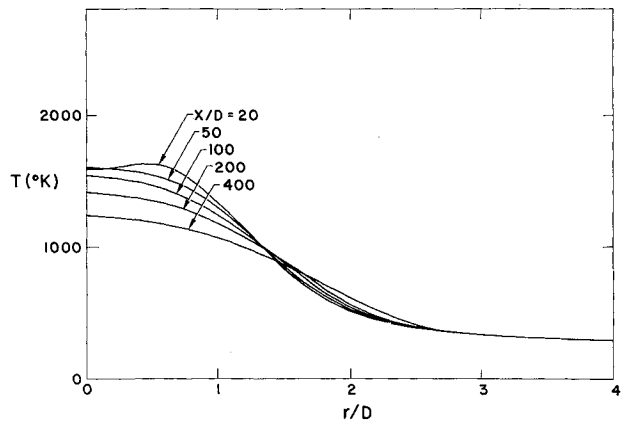

Fig. 7 The cooling of the wake by heat conduction, shown by temperature profiles at various distances behind the body.

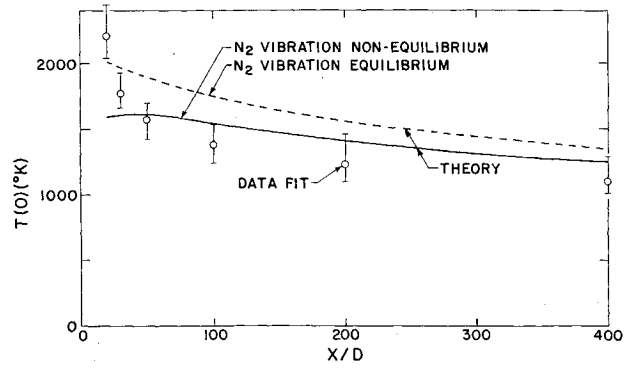

Fig. 8 Cooling of the wake along the centerline. The abscissa is the distance behind the sphere in body diameters. The points are the heights of gaussian temperature profiles which best fit the measured radiation. The error bars represent the scatter of the data.

or subsequent radial temperature profiles. This is in contrast to the work of Feldman who had assumed gaussian profiles. The profiles calculated in this way are plotted in Fig. 7 for various distances behind the body. The resulting curves are not quite gaussian; the profile for $X/D = 200$ is 5% higher at its shoulder than a gaussian fitted at the peak and $1/e$ points.

The variation of the centerline temperature $T(0)$ with X/D is given by the solid curve in Fig. 8. Because of the initial off-axis peak, the temperature rises slightly before decaying. (If the nitrogen vibration is relaxed by the CO_2 in the expansion region, then one must use the dotted curve in Fig. 6 as the initial condition for the cooling calculation. The resulting centerline temperatures are given by the dotted line in Fig. 8.) The curve in Fig. 9 shows the gradual increase of a, the $1/e$ width of the theoretical temperature profiles $T(r)$, defined by the relation

$$T(a) = [T(0) - 300°\text{K}]/e + 300°\text{K}$$

C. CO_2 Dissociation

When this experiment was begun, the available data[15] indicated a rather slow rate of dissociation for CO_2 up to 2730°K. Recently, however, experiments have been reported on CO_2 dissociation at higher temperatures.[16, 17] These results indicate that the dissociation of CO_2 proceeds quite quickly behind the blunt portions of the bow shock of the spheres fired in this experiment.

An estimate of these effects was made on the basis of the reaction

$$CO_2 + N_2 \underset{k_r}{\overset{k_d}{\rightleftharpoons}} CO + O + N_2 \qquad (2)$$

The reaction $2O \rightarrow O_2$ and the reactions of O atoms with the

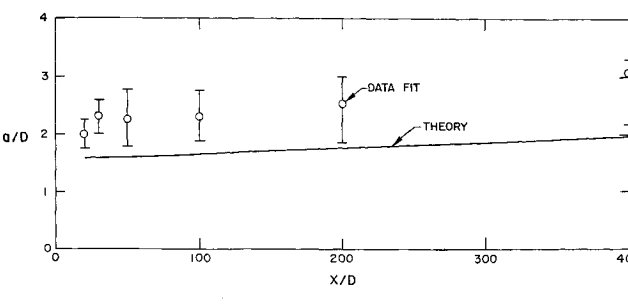

Fig. 9 Wake growth. The ordinate a is the $1/e$ width of the temperature profiles. The points are the widths of gaussian profiles which best fit the measurements.

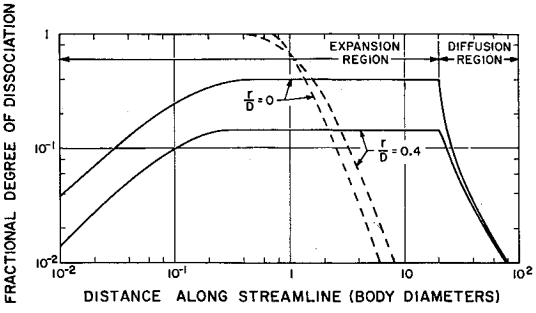

Fig. 10 Dissociation of CO_2 in the flow field of a sphere. The results of a nonequilibrium calculation are given by the solid lines; the dashed lines show the equilibrium values. In the expansion region, the dissociation is shown along two streamlines whose distance off the axis at $X/D = 20$ is given. In the diffusion region these values for r/D are held constant.

N_2, which may follow the CO_2 dissociation, were not included in the calculation. The dissociation rate k_d has been measured by Davies[17] for CO_2 dissociation in nitrogen at temperatures between 3500° and 6000°K. He fitted his data with the Arrhenius equation

$$k_d = 2.45 \times 10^{11} T^{1/2} \exp(-37{,}500°\text{K}/T) \text{ sec}^{-1} (\text{moles/cm}^3)^{-1}$$

which we have used to extrapolate the dissociation to higher and lower temperatures. (An expression from classical collision theory, which fitted the data just as well, would have given different values outside the temperature range of the measurements.) The recombination rate k_r has not been measured directly; therefore, it was calculated from k_d and the equilibrium constant[18] for reaction (2).

The differential equation for the variation of CO_2 concentration due to this reaction was integrated along streamlines in the expansion region using a Runge-Kutta scheme. The gas density and temperature histories were taken from the previously described chemistry program for 100% N_2; the effect of dissociation of CO_2 (which was initially only 5% of the gas mixture) on the temperature was not included. The results in the expansion region are shown by the solid curves in Fig. 10 for two streamlines. The curves are labeled by their distance away from the axis at the end of the expansion region (20 diam behind the body). On other streamlines farther off the axis, the degree of dissociation was less than 1%. The figure also shows the degree of dissociation which would be reached if the reaction had reached equilibrium at each point.

The calculation shows that immediately behind the bow shock the CO_2 starts to dissociate but as the gas expands at the shoulder of the body the level of dissociation becomes frozen. The rate of recombination is negligible even after the equilibrium degree of dissociation has fallen below 1%.

Because of the appreciable concentration gradients perpendicular to the wake axis, the degree of dissociation near the axis will be reduced due to diffusion. To study this effect, the diffusion of the undissociated CO_2 molecules in the direction of the axis was calculated. A computer program very similar to the one used to integrate Eq. (1) for wake cooling was employed. The diffusion calculation started at $X/D = 20$ (where ambient pressure is reached), and the results of the streamtube calculation described previously were used as the initial condition. The results of the diffusion calculation are shown in Fig. 10 both on the axis and 0.4 diam off the axis. In the diffusion region the value of r/D is held constant for each curve shown (we are no longer following streamlines here). In this region the ordinate gives the relative amount by which the mole fraction of CO_2 is reduced below its original value. It is evident that the CO_2 diffuses rapidly. At 30 diam behind the body, the CO_2 concentration is depressed by only 7%.

The CO (which was produced by the dissociation of CO_2) diffuses away from the axis at the same time. Its diffusion coefficient is about the same as that of CO_2 (it is actually slightly larger), so in the diffusion region the ordinate of Fig. 10 retains approximately the same definition that it had in the expansion region, namely, $[CO]/([CO] + [CO_2])$.

The sharp knee at 20 diam in Fig. 10 shows that the separation of the flow field into regions of pure expansion and pure diffusion, which was reasonable for temperature calculations, is inappropriate for an accurate calculation of species concentration. The results shown are merely an upper limit to the maximum amount of dissociation. If diffusion had been included in the region where the gas is still expanding, the apparent degree of dissociation would have been lowered sooner than shown in Fig. 10. We conclude that the CO_2 concentration may be considered restored to its original 5% concentration (to the accuracy with which radiation intensity can be measured in this experiment) by about 20 to 25 diam behind the body.

IV. Properties of CO_2

In this section a brief survey of CO_2 infrared radiation and vibrational relaxation is presented. Additional references and a more detailed discussion are given in Ref. 7.

A. CO_2 Infrared Radiation

The infrared detector used in this experiment, together with a filter, viewed a portion of the 4.3-μ band of CO_2 which contains thousands of spectral lines. A variety of mathematical models exist which may be used to calculate the band radiation from homogeneous gas samples with reasonable accuracy for a wide range of conditions. (Plass[19, 20] has given useful discussions of these approximations.) Such simple procedures may be applied to inhomogeneous gas samples such as the wake that we are considering only if the self-absorption of radiation within the gas sample is negligible.

Plass[20] has analyzed self-absorption in terms of two dimensionless parameters x and β, defined by

$$x \equiv Spl/2\pi\alpha = (S/2\pi\alpha_0)cl \tag{3}$$

and

$$\beta \equiv 2\pi\alpha/d = (2\pi\alpha_0/d)p_t \tag{4}$$

Here S is the average strength of the spectral lines over the spectral interval viewed; d is their average spacing in (centimeters)$^{-1}$; p is the partial pressure of the radiating species in atmospheres; $c = p/p_t$ is its fractional concentration; p_t is the total gas pressure in atmospheres; l is the thickness of the homogeneous gas sample in centimeters; $\alpha = \alpha_0 p_t$ is the half-width at half amplitude, in (centimeters)$^{-1}$, of the spectral lines, which we assume for the present to have pure Lorentz line shape. Plass has shown that there is less than 10% self-absorption within a gas sample if the following criteria are satisfied: $x < 0.2$ and $\beta x < 0.2$. (This analysis is based on the use of either the Elsasser model or the uniform statistical model of band radiation.[19]) If both of these inequalities are satisfied, then the emissivity of a homogeneous gas sample is given, to 10% accuracy or better, by the linear approximation

$$\epsilon = \beta x = (S/d)pl \tag{5}$$

where pl is the optical thickness of the gas sample.

The region of validity of the linear approximation is indicated by the unshaded area of Fig. 11. If $\beta x > 0.2$, then significant self-absorption due to overlapping of spectral lines occurs. If $x > 0.2$, then self-absorption at the centers of individual lines becomes important.

In the linear region important simplifications are possible. First, the emissivity of gas of a given optical thickness pl depends only upon S/d, i.e., upon the strengths of the lines and their spacing; it is independent of the line shape. Thus Eq. (5) may also be used for lines of pure Doppler contour, or

for mixed Doppler and Lorentz shapes. Second, the treatment of inhomogeneous gas samples is simple in the linear region. Because self-absorption is negligible, the total emission is simply the sum of the emission from all parts of the gas along the line of sight:

$$\epsilon = \int (S/d) p dl$$

(In this integral, S/d and p may be variable functions of position.) We will show later that this simplification is indeed allowable for the conditions of this experiment. Otherwise, analysis of the radiation from a wake, which is not all at the same temperature, would be very difficult, since the general problem of emission from an inhomogeneous gas sample over a finite spectral interval has not been solved.

The quantities $S/2\pi\alpha_0$, $2\pi\alpha_0/d$, and S/d appearing in Eqs. (3–5) may be obtained from calculations by Malkmus[21] of the spectral emission from the 4.3-μ band of CO_2 up to 3000°K. These calculations have been extensively checked by a variety of experimental techniques.[22–25]

We first use Malkmus' results to show the validity of the linear approximation [Eq. (5)] in this experiment. For the conditions in the ballistic range, we have $c = 0.05$ and $p_t = 0.0132$ atm. A homogeneous gas sample whose thickness matches the full width of the wake would have $l \approx 2$ cm. The wave number of the center of the interference filter is $\nu = 2280$ cm^{-1}. Values of β and x calculated for these conditions as a function of temperature are plotted on Fig. 11.

The calculated points all lie within the linear region but approach its boundary at 600°K, where $x = 0.15$ for $l = 2$ cm. There is no danger of lines overlapping at that point, but there may be slight absorption at line centers. It can be shown that in this case Eq. (5) is accurate to 7.5%.

At these low pressures Doppler broadening cannot be neglected. However, the addition of Doppler effects will simply lower the strengths of the lines at their centers and increase them at the wings. Hence our chief worry, possible absorption at line centers, is reduced by Doppler broadening. We would not intuitively expect trouble from overlapping of Doppler broadened lines either, since the $\beta x = 0.2$ boundary on Fig. 11 is so far away. Indeed, it can be shown on the basis of Plass' work[19] that, if self-absorption due to overlapping of pure Lorentz lines is negligible, it is also negligible for pure Doppler lines.

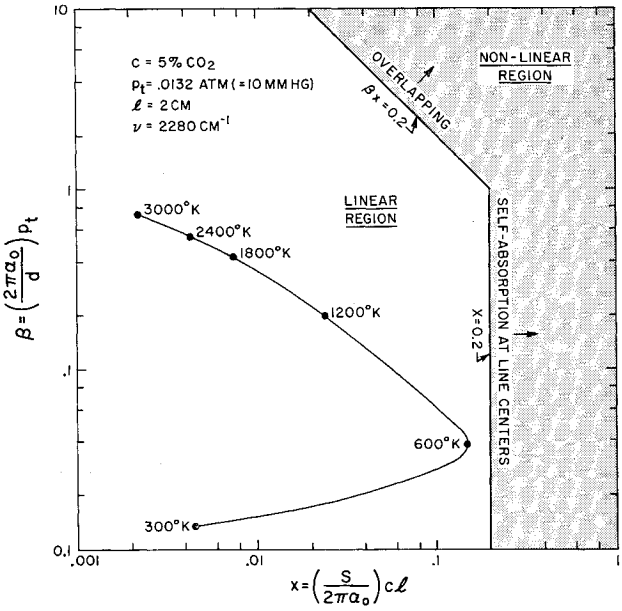

Fig. 11 Map of the linear region (unshaded area) of emission from a band of spectral lines, where self-absorption of emitted radiation causes an effect of less than 10%, for the Elsasser model or the uniform statistical model. The parameters x and β are defined by Eqs. (3) and (4). The points are calculated for CO_2 under the conditions listed and show that, for that case, self-absorption is negligible.

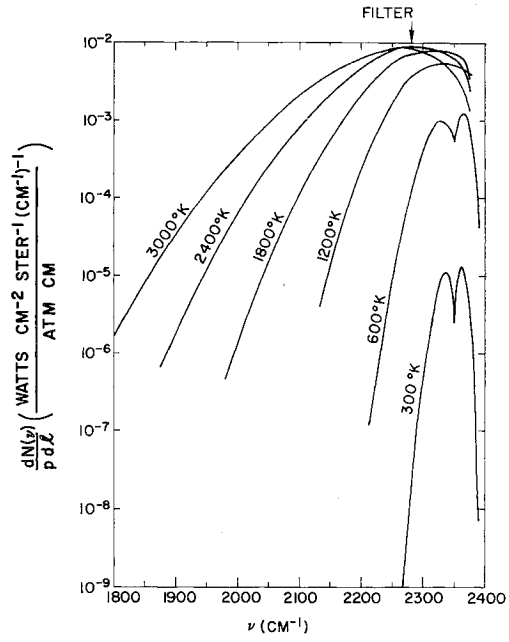

Fig. 12 Spectral radiance $N(\nu)$ per unit of optical thickness pl obtained from Malkmus calculations. The spectral location of the interference filter used is shown.

If Malkmus' result for S/d is multiplied by $N°(\nu)$, the spectral radiance of a blackbody (in w/cm^2-sr-cm^{-1}), we obtain $dN(\nu)/pdl$, the spectral radiance per unit optical thickness of CO_2 in the 4.3-μ region. The latter quantity is shown in Fig. 12, along with the spectral location of the interference filter used.

This figure shows that CO_2 (as viewed through the filter) is a fairly sensitive thermometer at 1200°K, where a 10% change of temperature produces a 25% change in radiance. The sensitivity gradually decreases to zero, however, at about 2600°K. For higher temperatures, a longer wavelength filter could be used. (A two-color temperature measurement could be made by measuring the ratio of the radiations from CO_2 at two different wavelengths. An attempt to do this in this experiment was frustrated because the second spectral channel used (at 2210 cm^{-1}) was sensitive to radiation from CO, which is produced when some of the CO_2 dissociates.)

B. CO_2 Vibrational Relaxation

The rate of vibrational relaxation of CO_2 has been extensively studied.[15, 26–31] According to some of these experiments, the three modes of vibration of CO_2 relax together, whereas others indicate that the modes may have separate relaxation times. The ν_3 mode, which is responsible for the radiation observed in this experiment, may be studied individually by the spectrophone,[32–34] but the validity of that technique has yet to be fully established.

If the measured relaxation times are plotted[7] and the average trend of the data extrapolated to 1500°K, we obtain a relaxation time of about 40 μsec for pure CO_2 at the total pressure in the ballistic range, or a relaxation distance of 28 body diameters. Such a response time would be adequate for the present study of slowly varying temperatures. (These rates might be speeded up by a factor of 2 or so by water vapor in the concentrations that were possible in the ballistic range.)

The gas in the range is 95% N_2, however, which may possibly be less efficient than CO_2 for relaxation of other CO_2

molecules. Slobodskaia and Gasilevich, who studied the ν_3 mode with a spectrophone,[33] have found an indication of such an effect, but this conclusion has not yet been verified elsewhere.† Camac[35] has recently studied the vibrational relaxation of CO_2 in a low-density shock tube. He concludes that all modes of CO_2 vibration relax together with a single time constant.

V. Results

For the most direct comparison of theory and experiment, we have calculated the infrared radiance of the wake (in w/cm²-sr) from the theoretical temperature profiles $T(r)$ given in Fig. 7. For several values of y (the lateral distance between the optical axis of the infrared detecting system and the wake axis) the radiation was integrated along the path shown in Fig. 2. In making these integrations it was assumed that: 1) the total pressure was at ambient level; 2) the fractional concentration of CO_2 was at its original value (5%); and 3) the vibrational temperature of CO_2 was equal to the translational temperature.

Examples of the resulting radiance profiles $N(y)$ are shown by the solid lines in Figs. 3 and 4. At 20 body diameters behind the sphere, the observed radiation exceeds the amount expected by a factor of 2 or more. At 200 body diameters the agreement between the calculated and observed radiance profiles is very good for small values of y, but the observed profile is wider than the theoretical one. It is physically more interesting, however, to compare theory and experiment in terms of temperature. For this purpose gaussian radial temperature profiles of the form

$$T(r) = [T(0) - 300°\text{K}] \exp[-(r/a)^2] + 300°\text{K}$$

were used. The height $T(0)$ and the width a were adjusted for the best fit to the measured radiance profile $N(y)$. The dashed line in Fig. 4 is an example of the closeness of fit to the data that can be obtained.

The centerline temperatures derived from this two-parameter fit to the measurements are shown as data points in Fig. 8 for various distances behind the body. The agreement between these experimentally determined CO_2 vibrational temperatures and the calculated translational temperatures is best at 50 body diameters or more behind the sphere. In that region, the experimental values lie within about 150°K of the theoretical curve and have a spread of about ±150°K.

In the near wake, between 20 and 50 diam behind the sphere, we see that the experimentally determined vibrational temperatures start out about 600°K above the theoretical values (whereas the data scatter corresponds to only about ±200°K) and decrease much more rapidly with X than can be accounted for by heat conduction alone.

The excess radiation seen might be explained by assuming that the pressure is about 1.5 to 2 times ambient value at $X/D = 20$, and decays to ambient value only at about $X/D = 50$. This conclusion would be in contradiction to Lukasiewicz's correlation[13] of pressure decay, which has not yet been verified experimentally at high Mach numbers and high enthalpy. The experimental values of the wake widths are shown in Fig. 9. They are about 50% greater than the theoretical values.

VI. Conclusions

Infrared radiation from CO_2 has been shown to give a reasonably accurate measure of the temperature over an extensive region of the wake. Thus, one is encouraged to consider extensions and improvements of the infrared technique.

One awkward aspect of the present study is that the CO_2 tracer gas travels through a very hot region in the vicinity of the body en route to the much cooler wake. A more detailed study of the resulting CO_2 chemistry than that given in this paper would be possible, but would not be very relevant to our main field of interest: the flow of air and its components around hypersonic projectiles and in their wakes. Therefore, the most fruitful continuation of this work with blunt bodies would probably be the infrared study of NO produced by such projectiles traveling at re-entry velocity in air in a ballistic range. Here the chemistry involved would be of more practical interest.

Another promising application of the infrared technique would be to the wake of slender bodies. Here the temperatures around the body are much lower. A calculation similar to that described previously shows that there will be very little dissociation of CO_2 in the vicinity of a 1-in.-long sharp cone traveling at 15,000 fps, for example. Thus the use of CO_2 as a thermometer to measure the temperature of the near wake of a pointed cone in a ballistic range, for example, should be more straightforward than in the present measurement.

† Since the completion of the present work the writer has made some shock-tube measurements of the rate of excitation of the ν_3 mode of CO_2 in 5% CO_2-95% N_2 mixtures over the temperature range 1300–3200°K. The CO_2 emission at 4.7 μ was monitored. The preliminary results of these measurements, scaled to the conditions of the present experiment, give a relaxation distance of about 80 body diameters at 1500°K.

References

[1] Hansen, C. F., Primich, R. I., Steinberg, M., and Maiden, C. J., "Measurements and analysis of optical and microwave observables in flow about hypersonic models," AIAA Preprint 63-204 (June 1963).

[2] "Status report on the re-entry physics program, December 31, 1962," Canadian Research and Development Establishment Tech. Memo. 740/63 (April 1963).

[3] Taylor, R. L., Keck, J. C., Melcher, B. W., II, and Carbone, R. M., "A high speed scanner for transverse radiation measurements of luminous hypersonic wakes," Avco-Everett Research Lab. Research Rept. 155 (March 1963); also AIAA J. **1**, 2186–2188 (1963).

[4] Taylor, R. L., Melcher, B. W., II, and Washburn, W. K., "Measurements of the growth and symmetry of the luminous hypersonic wake behind blunt bodies," Avco-Everett Research Lab. Research Rept. 163 (May 1963); also "Studies of the luminous hypersonic wake," AIAA J. **2**, 1731–1738 (October 1964).

[5] Hooker, W. J., "Preliminary hypervelocity wake brightness temperature measurements," General Dynamics/Astronautics, Spaces Sciences Lab. Rept. GDA 63-0506 (October 1963).

[6] Muntz, E. P. and Zempel, R. E., "Slender body near wake density measurements at Mach numbers thirteen and eighteen," General Electric Space Sciences Lab. Doc. 63SD718 (July 1963); also AIAA Preprint 63-272 (June 1963).

[7] Young, L. A., "Infrared temperature measurement of the laminar wake of a hypersonic sphere," Avco-Everett Research Lab. Research Rept. 179 (May 1964).

[8] Hidalgo, H., Taylor, R. L., and Keck, J. C., "Transition in the viscous wake of blunt bodies at hypersonic speeds," Avco-Everett Research Lab. Research Rept. 133 (April 1961); also J. Aerospace Sci. **29**, 1306–1315 (1962).

[9] Feldman, S., "Trails of axi-symmetric hypersonic blunt bodies flying through the atmosphere," Avco-Everett Research Lab. Research Rept. 82 (December 1959); also J. Aerospace Sci. **28**, 433–448 (1961).

[10] Lykoudis, P. S., "Laminar hypersonic trail in the expansion-conduction region," AIAA J. **1**, 772–775 (1963).

[11] Lobb, R. K., "Experimental measurement of shock detachment distance on spheres fired in air at hypervelocities," U. S. Naval Ordnance Lab. AGARD Paper (April 1962).

[12] Lin, S. C. and Teare, J. D., "A streamtube approximation for calculation of reaction rates in the inviscid flow field of hypersonic objects," *Sixth Symposium on Ballistic Missile and Aerospace Technology* (Academic Press Inc., New York, 1961), Vol. 4, pp. 35–50; also Avco-Everett Research Lab. Rept. AMP 77 (August 1961).

[13] Lukasiewicz, J., "Hypersonic flow-blast analogy," Arnold Engineering Development Center Rept. TR-61-4 (June 1961); also ARS Preprint 2169-61 (October 1961).

[14] Hansen, C. F., "Approximations for the thermodynamic and transport properties of high-temperature air," NASA TR R-50 (1959).

[15] Gaydon, A. G. and Hurle, I. R., "Measurement of times of vibrational relaxation and dissociation behind shock waves in N_2, O_2, air, CO, CO_2 and H_2," *Eighth Symposium on Combustion, 1960* (The Combustion Institute, Baltimore, Md., 1962), pp. 309–318.

[16] Brabbs, T. A., Belles, F. E., and Zlatarich, S. A., "Shock-tube study of carbon dioxide dissociation rate," J. Chem. Phys. **38,** 1939–1944 (1963).

[17] Davies, W. O., "Radiative energy transfer on entry into Mars and Venus," IIT Research Institute Rept. IITRI-T200-6 (October 1963); also "Carbon dissociation at 3500° to 6000°K," J. Chem. Phys. **41,** 1846–1852 (1964).

[18] Gray, D. E. (ed.), *American Institute of Physics Handbook* (McGraw-Hill Book Co., Inc., New York, 1963), 2nd ed., pp. 4-315–4-330.

[19] Plass, G. N., "Models for spectral band absorption," J. Opt. Soc. Am. **48,** 690–703 (1958).

[20] Plass, G. N., "Useful representations for measurements of spectral band absorption," J. Opt. Soc. Am. **50,** 868–875 (1960).

[21] Malkmus, W., "Infrared emissivity of carbon dioxide (4.3-μ band)," J. Opt. Soc. Am. **53,** 951–961 (1963); also General Dynamics/Astronautics Rept. AE62-0204 (February 1962).

[22] Ferriso, C. C., "High-temperature spectral absorption of the 4.3-micron CO_2 band," J. Chem. Phys. **37,** 1955–1961 (1962).

[23] Steinberg, M. and Davies, W. O., "High-temperature absorption of carbon dioxide at 4.40 μ," J. Chem. Phys. **34,** 1373–1377 (1961).

[24] Oppenheim, U. P. and Ben-Aryeh, Y., "Statistical model applied to the region of the ν_3 fundamental of CO_2 at 1200°K," J. Opt. Soc. Am. **53,** 344–350 (1963).

[25] Sulzmann, K. G. P., "High temperature shock tube CO_2–transmission measurements at 4.25μ," J. Quant. Spectry. Radiative Transfer **4,** 375–413 (1964).

[26] Herzfeld, K. F. and Litovitz, T. A., *Absorption and Dispersion of Ultrasonic Waves* (Academic Press Inc., New York, 1959), pp. 246–250.

[27] Smiley, E. F. and Winkler, E. H., "Shock-tube measurements of vibrational relaxation," J. Chem. Phys. **22,** 2018–2022 (1954).

[28] Griffith, W., Brickl, D., and Blackman, V., "Structure of shock waves in polyatomic gases," Phys. Rev. **102,** 1209–1216 (1956).

[29] Daen, J. and de Boer, P. C. T., "Some studies on argon, helium, and carbon dioxide with an integrated-schlieren instrumented shock tube," J. Chem. Phys. **36,** 1222–1228 (1962).

[30] Johannesen, N. H., Zienkiewicz, H. K., Blythe, P. A., and Gerrard, J. H., "Experimental and theoretical analysis of vibrational relaxation regions in carbon dioxide," J. Fluid Mech. **13,** 213–224 (1962); also Zienkiewicz, H. K., Johannesen, N. H., and Gerrard, J. H., "Further results on the over-all density ratios of shock waves in carbon dioxide," J. Fluid Mech. **17,** 267–270 (1963).

[31] Witteman, W. J., "Vibrational relaxation in carbon dioxide. II," J. Chem. Phys. **37,** 655–661 (1962).

[32] Slobodskaia, P. V., Izv. Akad. Nauk SSSR, Ser. Fiz. **12,** 656 (1948); quoted in Ref. 26.

[33] Slobodskaia, P. V. and Gasilevich, E. S., "Development of a method of determining the relaxation time of the vibratory state of molecules using a spectrophone," Opt. Spectry. (USSR) (English transl.) **7,** 58–62 (1959).

[34] Jacox, M. E. and Bauer, S. H., "Collisional energy exchange in gases. Use of the Spectrophone for studying relaxation processes in carbon dioxide," J. Phys. Chem. **61,** 833–844 (1957).

[35] Camac, M., "CO_2 relaxation processes in shock waves," Avco-Everett Research Lab. Research Rept. 194 (October 1964).

APRIL 1965 AIAA JOURNAL VOL. 3, NO. 4

Unsteady Three-Dimensional Laminar Jet Mixing of a Compressible Fluid

S. I. Pai*
University of Maryland, College Park, Md.

The fundamental equations of an unsteady three-dimensional laminar jet mixing of a compressible fluid have been discussed. These equations are simplified by introducing two stream functions. Finally, the unsteady jet flow that deviates slightly from an unsteady uniform flow is studied in detail. It was found that, for arbitrary three-dimensional jets, the velocity and temperature distributions tend to be axisymmetrical at large time-from-start and far downstream. Some numerical examples are given.

I. Introduction

MOST of the free jet-mixing problems consider the cases of steady flow[2] of two-dimensional or axisymmetrical or rotationally symmetrical[3–5] configuration in which the flow variables are functions of two spatial variables only. Little has been done for the case of general three-dimensional flow in which the flow variables are functions of all three spatial variables as well as time. In practice, the jet flow may oscillate, and the general stream in which the jet flow is located may be unsteady itself. Furthermore, the directions of the general stream and of the jet may not be the same. Hence, the three-dimensional character of the jet-mixing problem is important. In this paper, we discuss the general behavior of an unsteady three-dimensional jet-mixing region in a uniform stream of a viscous and compressible ideal gas.

We consider a jet issuing from a nozzle into an unsteady freestream. The deviation of the direction of the jet from that of the freestream is assumed to be small. We further assume that the deviation of the cross section of the exit of the nozzle from a circular cross section is also small. As a result, the radial component of the jet flow will be small, and the jet behaves as a free boundary-layer flow with a large gradient in the radial (r) direction. If we take x as the direc-

Received June 4, 1964; revision received December 31, 1964. This research was supported in part by the U.S. Air Force through the Air Force Office of Scientific Research under Grant No. AFOSR 141-65. The numerical computations were carried out in the Computer Sciences Center, University of Maryland by H. H. Chu.

* Research Professor, Institute for Fluid Dynamics and Applied Mathematics. Associate Fellow Member AIAA.